

Detection of Cardiac Infarction in MRI C-SENC Images

Ahmad O. Alghary
Senior Biomed S/W Eng
Diagnosoft Inc
Cairo Intl Office, Egypt
ahmad.alghary@diagno
soft.com

Ahmed M. El-Bialy
Systems and Biomedical
Eng. Dept., Faculty of
Engineering
Cairo Univ., Giza, Egypt
Abialy_86@yahoo.com

Ahmed H. Kandil
Systems and Biomedical
Eng. Dept., Faculty of
Engineering
Cairo Univ., Giza, Egypt
Ahkandil_1@yahoo.com

Nael F. Osman
Radiology Department,
School of Medicine
Johns Hopkins
University, Baltimore,
North Carolina, USA

Abstract— Composite Strain Encoding (C-SENC) is an Magnetic Resonance Imaging (MRI) technique for acquiring simultaneous viability and functional and images of the heart. It combines two imaging techniques, Delayed Enhancement (DE) and Strain Encoding (SENC). In this work, a novel multi-stage method is proposed to identify ventricular infarction in the functional and viability images provided by C-SENC MRI. The proposed method is based on sequential application of Otsu's thresholding, morphological opening, square boundary tracing and the subtractive clustering algorithm. This method is tested on images of ten patients with and without myocardial infarction (MI). The resulting clustered images are compared with those marked up by expert cardiologists who assisted in validating results coming from the proposed method. Infarcted tissues are correctly identified using the proposed method with high levels of sensitivity and specificity.

Keywords- Infarction; C-SENC MRI; Delayed Enhancement; styling; insert (key words)

I. INTRODUCTION

ACCURATE identification of myocardial infarction (MI) is considered critical for therapeutical decision-making [1]. Functional images are useful in determining the contractility patterns in the affected regions [1]. On the other hand, viability images are used to differentiate between viable and nonviable tissues [3].

By combining the information of functionality and viability, myocardial tissue can be classified into three identifiable types: (i) normally contracting tissue, which represents normal myocardium; (ii) non-contracting yet viable tissue, which represents hibernating myocardium; and (iii) non-viable tissue, which represents infarcted myocardium [4].

Previously, a method was proposed to identify different heart tissues from MRI C-SENC images using an unsupervised multi-stage clustering technique [5]. The method was based on sequential application of the Fuzzy C-means (FCM) and iterative self-organizing data (ISODATA) clustering algorithms. In a more recent work, Bayesian classifier was proposed to identify the background region, then the filtered tissue regions were classified into the different tissue types using FCM algorithm [6].

In this work, a novel, automatic, multi-stage method is proposed to identify different heart tissues from tuned images provided by Cardiac Magnetic Resonance (CMR) Composite Strain Encoding (C-SENC) images of transverse sections of the left ventricle (LV), and to identify infarcted myocardial tissues. This method is based on the application of Otsu's thresholding technique, morphological opening, square boundary tracing and the subtractive clustering algorithm. Numerical simulations, real CMR images of patients and expert cardiologists' markings were used to validate the proposed method, which showed excellent results with respect to sensitivity and specificity.

II. THEORY

A. C-SENC

Recently, the Composite Strain Encoding (C-SENC) MRI technique has been introduced for simultaneous cardiac functional and viability imaging in a single short breathhold [1]. No additional time, when compared with standard Delayed Enhancement (DE) viability imaging, is required for acquiring the additional functional images. This technique results in three images: no-tuning (NT), low-tuning (LT), and high-tuning (HT). Bright regions in the NT, LT, and HT images represent infarction (or blood), akinetic, and contracting tissues, respectively. An anatomy (ANAT) image of the heart can also be constructed by adding the LT and HT images as described in 0 to show the anatomical structure of the heart (both contracting and non-contracting myocardium) with no signal from blood. Figure 1 shows an example of acquired C-SENC images.

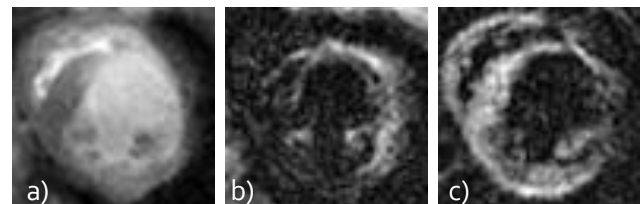


Figure 1. C-SENC Images of a patient suffering myocardial infarction: a) NT, b) LT, c) HT

Table I shows the signal intensities in C-SENC images for the blood, background, and the different tissue types.

B. Otsu Thresholding

Thresholding is a well-known technique for image segmentation that tries to identify and extract a target from its background on the basis of the distribution of gray levels in image objects. Otsu's method chooses the optimal thresholds by maximizing the between-class variance with an exhaustive search [7].

Reference [8] concluded that Otsu's method was one of the

TABLE I
TISSUE TYPES OCCUPY DIFFERENT AND THEIR CHARACTERISTIC SIGNAL INTENSITIES IN THE USED IMAGES

Type	ANAT	NT	LT	HT
Blood	Low	High	Low	Low
Infarcted	High	High	High	Low
Functional	High	Medium	low	High
Background	Low	Low	Low	Low

Signal intensities of different tissues in the No-Tuning (NT), Anatomy (ANAT), and High-Tuning (HT) C-SENC images. High = signal intensities greater than 0.8 in normalized images; and Low = signal intensities less than 0.2 in normalized images.

best threshold selection methods for general real world images. Otsu's method uses an exhaustive search to evaluate the criterion for maximizing the between-class variance.

An image is a 2D grayscale intensity function, and contains N pixels with gray levels from 1 to L . The number of pixels with gray level i is denoted n_i , giving a probability of gray level i in an image of

$$p_i = n_i/N \quad (1)$$

In the case of bi-level thresholding of an image, the pixels are divided into two classes, C_1 with gray levels $[1, \dots, t]$ and C_2 with gray levels $[t+1, \dots, L]$. Then, the gray level probability distributions for the two classes are

$$C_1: p_1/\omega_1(t), \dots, p_t/\omega_1(t) \quad , \text{ and}$$

$$C_2: p_{t+1}/\omega_2(t), p_{t+2}/\omega_2(t) \dots p_L/\omega_2(t),$$

$$\text{where } \omega_1(t) = \sum_{i=1}^t p_i \quad (2)$$

$$\text{and } \omega_2(t) = \sum_{i=t+1}^L p_i \quad (3)$$

Also, the means for classes C_1 and C_2 are

$$\mu_1 = \sum_{i=1}^t i p_i / \omega_1(t) \quad , \text{ and} \quad (4)$$

$$\mu_2 = \sum_{i=t+1}^L i p_i / \omega_2(t) \quad (5)$$

Let μ_T be the mean intensity for the whole image. It is easy to show that

$$\omega_1 \mu_1 + \omega_2 \mu_2 = \mu_T \quad (6)$$

$$\mu_1 + \mu_2 = 1 \quad (7)$$

Otsu defined the between-class variance [7] of the thresholded image as

$$\sigma_B^2 = \omega_1 (\mu_1 - \mu_T)^2 + \omega_2 (\mu_2 - \mu_T)^2 \quad (8)$$

For bi-level thresholding, Otsu verified that the optimal threshold t^* is chosen so that the between-class variance σ_B^2 is maximized; that is,

$$t^* = \text{Arg Max}\{\sigma_B\} \quad \text{where} \quad 1 \leq t < L \quad (9)$$

C. Theo Pavlidis' Tracing Algorithm

This algorithm is one of the relatively recent contour tracing algorithms. It was proposed by Theo Pavlidis in 1982 [9]. In this algorithm, the contour is traced in a counterclockwise direction. This only affects the relative direction of movements while tracing the contour.

Given a digital binary image (a grid of black pixels, on a background of white pixels); a black pixel is located and declared as a "start" pixel. Locating a "start" pixel can be done in a number of ways; one of which is done by starting at the bottom left corner of the grid, scanning each column of pixels from the bottom going upwards until a black pixel is encountered.

Any black boundary pixel can be chosen to be the start pixel as long as its left adjacent pixel is white. Throughout the algorithm, the pixels of interest at any time are the three pixels: P_1 , P_2 and P_3 shown in Figure 2.

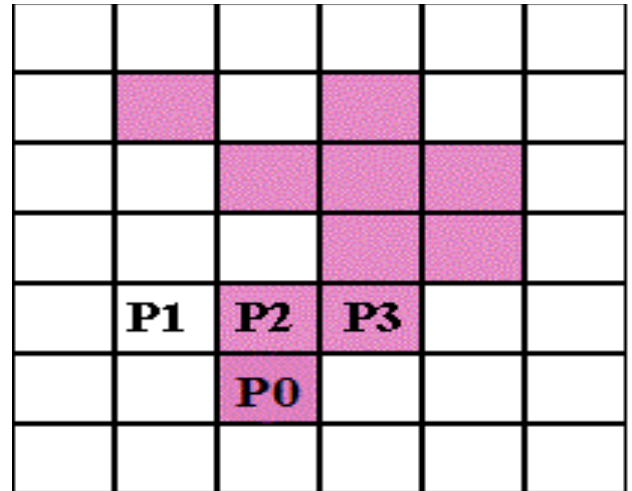


Figure 2. The three pixels of interest when scanning the pixel P0. P2 is the pixel in front of P0, P1 is the pixel adjacent to P2 from the left and P3 is the right adjacent pixel to P2.

The steps of the algorithm can be summarized as follows:

- When the current boundary pixel is P_0 , pixel P_1 is checked. If P_1 is black, then declare P_1 to be the current boundary pixel and move one step forward

followed by one step to the left to reach P1. Whereas if P1 is white proceed to check P2.

- If P2 is black, then P2 is declared to be the current boundary pixel. If P1 and P2 are white, check P3.
- If P3 is black, then P3 is declared to be the current boundary pixel.
- If all the three pixels (P1, P2, P3) in front of the current boundary pixel (P0) are white, then, rotate (while standing on the current boundary pixel) 90 degrees clockwise to face a new set of pixels in front of P0.
- Repeat the previous four steps until no black pixels are found or the current boundary pixel is the start one.

D. Subtractive Clustering

Subtractive clustering [10] uses the positions of the given data points to calculate a density function instead of calculating the density function at every possible position in the data space, thus reducing the number of calculations significantly. It uses data points as the candidates for cluster centers. However, the actual cluster centers are not necessarily located at one of the data points, but in most cases it is a good approximation.

Since each data point is a candidate for cluster centers, a density measure at data point x_i is defined as

$$D_i = \sum_{j=1}^n \exp\left(-\frac{\|x_i - x_j\|^2}{(r_a/2)^2}\right), \quad (10)$$

where r_a is a positive constant representing a neighborhood radius. Hence, a data point will have a high density value if it has many neighboring data points.

The first cluster center x_{c_1} is chosen as the point having the largest density value D_{c_1} . Next, the density measure of each data point x_i is revised as follows:

$$D_i = D_i - D_{c_1} \exp\left(-\frac{\|x_i - x_{c_1}\|^2}{(r_b/2)^2}\right), \quad (11)$$

where r_b is a positive constant which defines a neighborhood that has measurable reductions in density measure. Therefore, the data points near the first cluster center x_{c_1} will have significantly reduced density measure.

After revising the density function, the next cluster center is selected as the point having the greatest density value. This process continues until a sufficient number of clusters is attained.

III. MATERIALS AND METHODS

A. The Proposed Method

Figure 3 shows a sequence diagram of the proposed method, which consists of three main stages. The first stage of the proposed technique aims to detect and extract the left ventricle. This is done by the successive application of three sub-steps: thresholding, morphological opening and boundary detection.

Threshold grey-level intensity value is calculated using Otsu's thresholding. This value is applied to the ANAT image to binarize it and to differentiate pixels representing tissue from those representing background. Then, morphological opening is applied on the thresholded image. This aims to remove more noise pixels and to improve the myocardium boundaries so that they can be traced successfully in the next step. This step is applied for two successive times; the first time removes the small holes in the tissue while the second time does the same for the small holes in the background region.

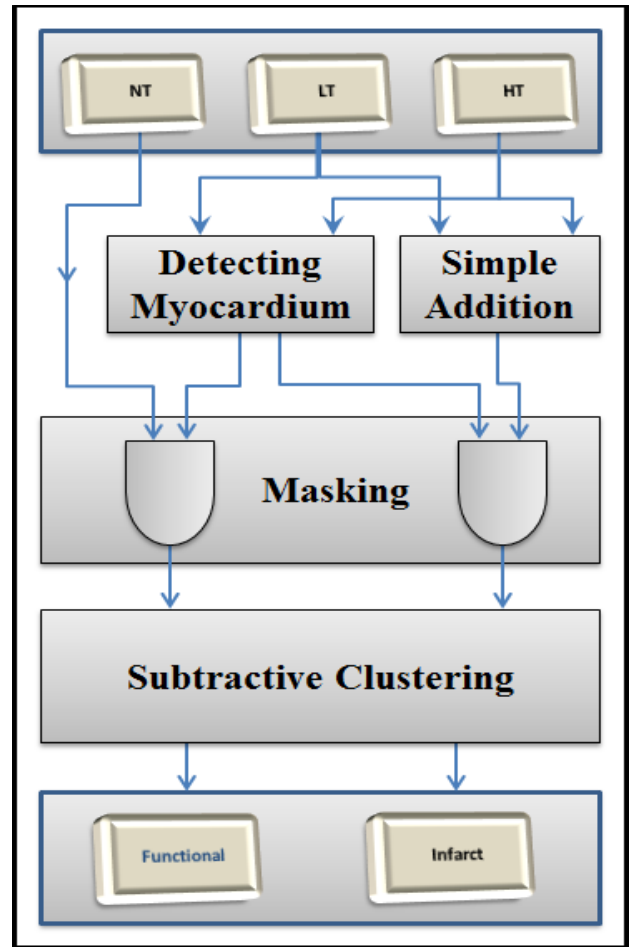


Figure 3. Stages of the Proposed Method

Finally, boundary detection is applied to select the left ventricular borders. This is done by using Theo Pavlidis' tracing algorithm [9]. All regions are traced, and then the most centralized region is selected to be the left ventricle as shown in Figure 4. This results in eliminating all regions that represent additional tissue areas.

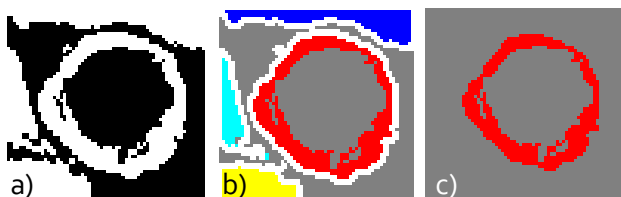


Figure 4. a) Morphologically opened image, b) image with boundary traced regions, c) Image showing the most centralized region that represents the left ventricle

In the second stage, the ANAT image of the heart is constructed by adding the LT and HT images as described in 0. Then, NT and ANAT Images are masked by the myocardium boundaries extracted in the second stage to exclude all pixels outside the left ventricle. This restricts the clustering to only two pixel types; functional and infarcted tissue. This is applied by ANDING the binary image that contains the pixels of the left ventricle only with the original ANAT and NT images, respectively. This results in two images (ANAT and NT) that contain only pixels corresponding to the left ventricular tissue.

The third stage of the proposed method consists of further clustering the myocardium through the application of subtractive clustering algorithm. In this stage, myocardium is classified into two major clusters: contracting and non-contracting tissue, from which we can extract the infarcted regions. Subtractive clustering detects the number of clusters and the central pixel of each one. This means preserving the method from failure when it is applied to real cases of fully functional heart, i.e. there is no infarcted tissue areas

B. Validation

A consultant cardiologist helped in the validation of the proposed method by marking the infarcted tissue regions in the real C-SENC MRI images. Infarcted regions were marked three times for each set. Infarctions extracted from the clustered images were compared with those extracted from the marked images on a pixel-by-pixel basis and statistical results were calculated. Figure 5 shows a colored scatter plot of the NT and ANAT images.

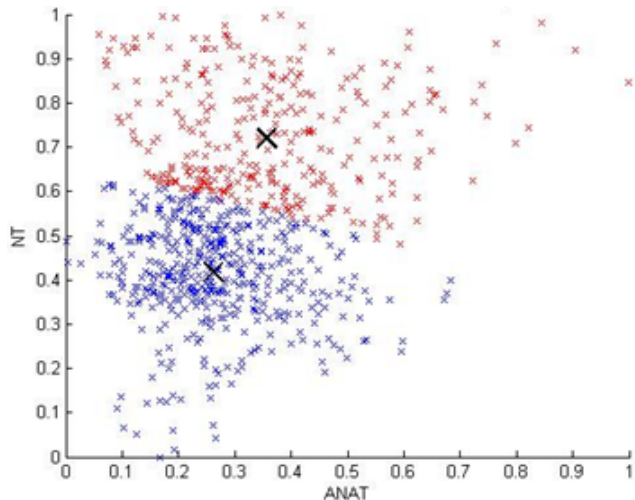


Figure 5. Fig. 5. Scatter plot of normalized NT and ANAT Images. The red scatters represent the infarcted pixels while the blue ones represent the function tissue.

IV. RESULTS

Figure 6 shows real short-axis C-SENC images and the resulting infarcted regions colored in red. The resulting images correctly identified the pixels marked as infarct with sensitivity of 90.19 – 98.38 % and specificity of 77.13 – 93.77 %. Quantitative performance and visual comparisons demonstrate the robustness of the proposed technique for identifying different tissue types.

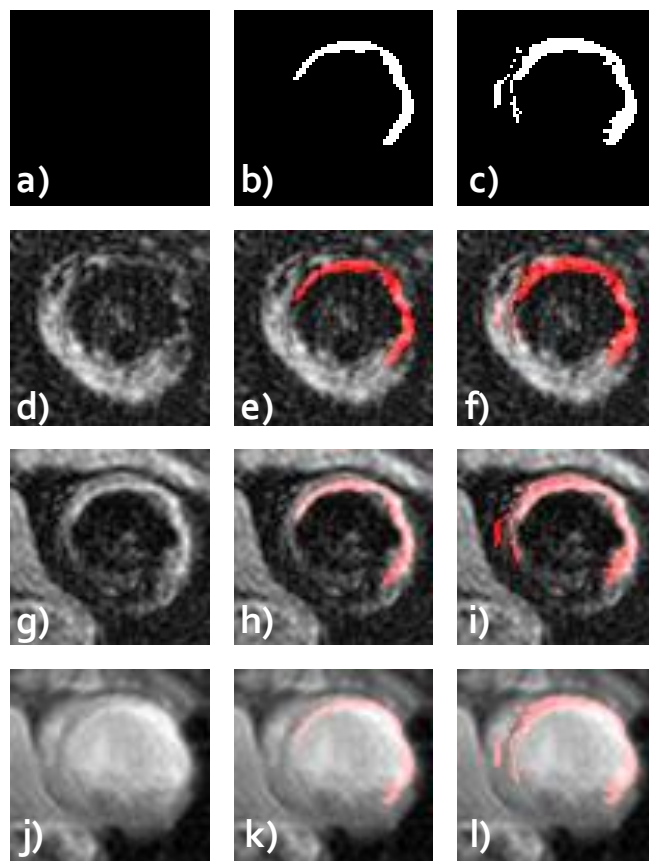


Figure 6. Representative C-SENC MRI images from a patient with myocardial infarction. The resulting infarcted regions are colored in red. The first column (d, g and j) shows a sample real images case, and the infarction map for the proposed technique. The second column (e, h and k) shows the markings of the consultant cardiologist. The third column (f, i and l) shows the resulting markings of the proposed method. Accuracy = 97.22%, Precision = 84.01%.

V. DISCUSSION AND CONCLUSION

The proposed technique was found to be robust in determining the existent infarction. Infarcted myocardium is specified only if there are enough data points in the infarct cluster during the application of the technique. For all the analyzed images, the technique correctly determines infarction existence.

One advantage of the resulting clustered images is the excellent removal of the blood due to the black-blood property in the LT and HT images. Thus, the resulting clustered images would allow for accurate measurement of the infarct size. Another advantage is that the proposed method can detect the number of clusters in the given images. This allows for successful detection of infarction absence.

Tissue of the myocardium detected as infarcted tissue indeed includes two clusters; infarct and hibernated (tissue that is not-contracting while still viable). It is clear that we are able to differentiate between contracting and non-contracting regions in the heart tissue, but still cannot differentiate between the hibernating and the infarcted tissue as both of them are non-contracting tissues. Further clustering may be applied to differentiate between these two regions.

In conclusion, a new method is proposed for identifying different heart tissues from C-SENC functional and viability images. The technique is based on the consecutive application of the Otsu's thresholding and subtractive clustering techniques. The method is successfully applied to transverse cross sectional images of the heart. It gives very good results regarding sensitivity and specificity although this type of images is known to suffer from high noise levels.

REFERENCES

[1] Ibrahim EH, Stuber M, Kraitchman DL, Weiss RG, Osman NF. Combined functional and viability cardiac MR imaging in a single breathhold. *Magn Reson Med* 2007; 58:843–849.
 [2] Osman NF, Sampath S, Atalar E, Prince JL. Imaging longitudinal cardiac strain on short-axis images using strain-encoding MRI. *Magn Reson Med* 2001; 46:324–334.

[3] Wu KC, Lima JA. Noninvasive imaging of myocardial viability: current techniques and future developments. *Circ Res* 2003; 93:1146–1158.
 [4] Watzinger N, Saeed M, Wendland MF, Akbari H, Lund G, Higgins CB. Myocardial viability: magnetic resonance assessment of functional reserve and tissue characterization. *J Cardiovasc Magn Reson* 2001; 3:195–208.
 [5] Ibrahim, E.-S.H., Weiss, R.G., Stuber, M., Spooner, A.E., Osman, N.F.: Identification of Different Heart Tissues from MRI C-SENC Images Using an unsupervised Multi-Stage Fuzzy Clustering Technique. *J. Magn. Reson. Imaging* 28(2), 519–526 (2008).
 [6] Motaal, A.G., El Gayar, N., Osman, N.F.: Automated Cardiac-Tissue Identification in Composite Strain-Encoded (C-SENC) Images Using Fuzzy C-means and Bayesian Classifier. *iCBBE*, Chengdu, China, 2010.
 [7] N. Otsu, A threshold selection method from gray-level histogram, *IEEE Transactions on System Man Cybernetics*, Vol. SMC-9, No. 1, 1979, pp. 62-66.
 [8] Neamat El Gayar, Friedhelm Schwenker, and Gunther Palm. A Study of the Robustness of KNN Classifiers Trained Using Soft Labels. *ANNPR* 2006, LNAI 4087, pp. 67–80, 2006.
 [9] T. Pavlidis, *Algorithms for Graphics and Image Processing*. Berlin, Germany: Springer Verlag, 1982, ch. 7.
 [10] Jang, J.-S. R., Sun, C.-T., Mizutani, E., *Neuro-Fuzzy and Soft Computing – A Computational Approach to Learning and Machine Intelligence*, Prentice Hall, 1997.